Chapter 2
What Should we Know about Electron Optics and the Construction of an Electron Microscope?

Abstract Whenever the term "electron microscope" used in this book then the transmission electron microscope is meant and not the (conventional) scanning electron microscope. The transmission electron microscope is a microscope in its true sense, i.e. an instrument for imaging of a sample that is transmitted and optically imaged by rays. Nevertheless, it is possible to focus and to scan the electron beam on the specimen in most of these devices, too ("STEM"—see Chap. 8). But it sticks to the transmission of the beam through the sample. In principle the transmission electron microscope is constructed like a (transmission) light optical microscope. Accordingly, we will deal with some electron-optical fundamentals, lens aberrations, and important components of the electron microscope in this chapter.

2.1 The Principle of Multistage Imaging

The useful magnification of a light optical microscope (and even more of an electron microscope) is reached by multistage imaging. Figure 2.1 shows this for the two-stage imaging of a light optical microscope.

In principle, an electron microscope is just constructed like a light optical microscope. However, it is turned upside down in most cases, i.e. the condenser is the lens on top.

For a system of two (thin) lenses with the focal lengths f_1 and f_2 as well as the distance t between them the total focal length f is

$$\frac{1}{f} = \frac{1}{f_1} + \frac{1}{f_2} - \frac{t}{f_1 \cdot f_2}. \tag{2.1}$$

Within an electron microscope the image distance b is given by the fixed positions of the lenses and the screen or the camera. Changing the focal length allows to image object planes being in different distances onto the screen (cf. the lens Eq. (1.3)). Later, we will see which capabilities can be opened by this.

The total magnification M of multistage imaging with the single magnification steps $M_1, M_2, \ldots M_n$ is given by

$$M = M_1 \cdot M_2 \cdot \ldots \cdot M_n. \tag{2.2}$$

J. Thomas, T. Gemming, *Analytical Transmission Electron Microscopy,*
DOI 10.1007/978-94-017-8601-0_2, © Springer Science+Business Media Dordrecht 2014

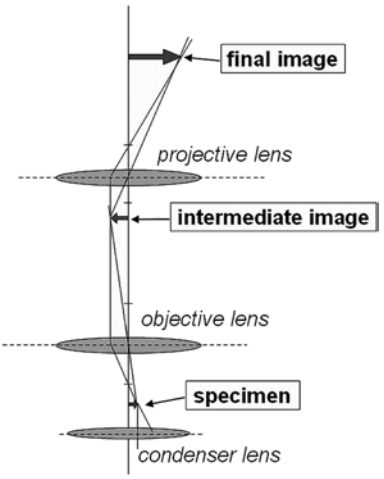

Fig. 2.1 Two-stage imaging at a light optical microscope. The light of the lamp (*arranged at the bottom*) penetrates a condenser lens and illuminates the specimen. The objective lens creates a magnified real intermediate image that is again magnified to the final image by the projective lens. The final image can be acquired by a photo plate, for example. Often, the projective is substituted by an eyepiece lens which allows seeing the magnified real intermediate image by eye with a loupe

In normal speech the magnification is often put on one level with the image ratio, although, properly speaking, these are two different things: The magnification is equal to the quotient of the visual angles with and without the optical device (1.2); the image ratio A_M is equal to the quotient of the image size y' and the object size y. A simple geometric reflection with consideration of the algebraic signs shows that A_M goes together with the negative quotient of image and object distance b and g, respectively. Finally, b can be calculated from g and the focal length f by the lens Eq. (1.3) and it follows:

$$A_M = \frac{y'}{y} = -\frac{b}{g} = \frac{f}{f-g}. \tag{2.3}$$

Looking at the algebraic sign the difference between magnification and image ratio can be most notably seen: Contrary to the magnification the image ratio can be positive or negative. A negative image ratio means that the image turns upside down. Taking only the modulus of the image ratio the value is the same as the magnification.

2.2 Rotational-Symmetric Magnetic Fields as Electron Lenses

Let us think about the following question: Why do the rotational-symmetric magnetic fields commonly used in electron microscopes work as electron lenses, i.e. why do they influence the electrons in the same way like glass lenses the light? Fig. 2.2 shows a sketch of the construction of such an electron lens.

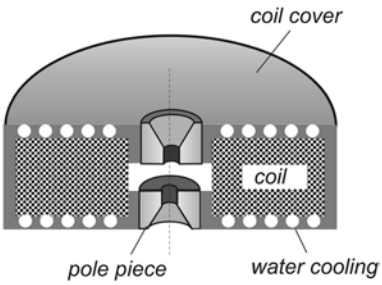

Fig. 2.2 Sketch of a magnetic electron lens. The coil current can reach up to 30 A. Water cooling causes the constant temperature within the lens. The pole piece shapes and concentrates the magnetic field

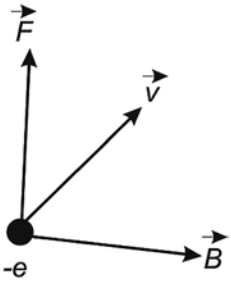

Fig. 2.3 Direction of the Lorentz force ***F*** concentrated on an electron with the charge –e moving with the velocity **v** within a magnetic field of induction **B**

For the desired lens effect all electrons which are not moving along the central axis ("optical axis") have to feel a power that moves them to this axis. We know that electrons moving with the velocity **v** within a magnetic field of strength (more precisely: of magnetic induction) **B** are influenced by the Lorentz force[1]

$$\mathbf{F} = -\mathrm{e} \cdot \mathbf{v} \times \mathbf{B} \tag{2.4}$$

with the elementary electric charge e. Additionally, it is considered that force **F**, velocity **v**, and magnetic induction **B** are vectors, i.e. they are denoted by modulus (numerical value) and direction. Commonly, such vectors are drawn by arrows with a length representing the modulus and an angle against a reference axis for representation of their direction. We are going to indicate a vector by a small arrow above the letter in the figures and by **bold letters** in equations and text.

How can we determine the direction of the Lorentz force following the "cross product" of Eq. (2.4)? In the mathematical sense **v**, **B**, and **F** create a "right-handed trihedron", i.e. the force **F** is perpendicular on the plane spanned by **v** and **B** (cf. Fig. 2.3).

Defining the direction we must not forget the negative sign in Eq. (2.4). For example, in practice one uses the "right-hand rule": *One spreads thumb, forefinger, and middle finger of the right hand so that they create a right angle against each other. Then one justifies the hand in such a way that the thumb points to the*

[1] Hendrik Antoon Lorentz, Dutch mathematician and physicist, 1853–1928, Nobel prize in physics in 1902

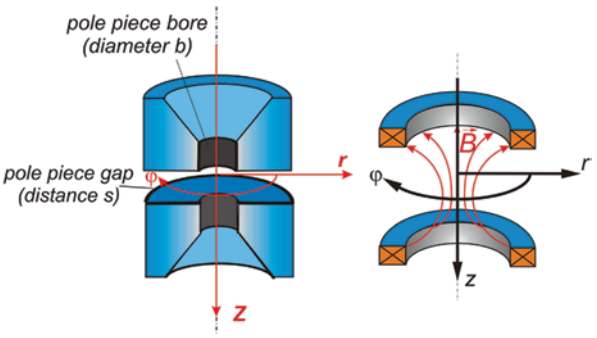

Fig. 2.4 Cylindrical coordinates in the region of the pole piece gap and field lines of the magnetic induction **B**

direction of the velocity and the forefinger to the direction of induction. In this case the middle finger points to the direction of the cross product (here: Lorentz force). Following this rule firstly we should get a force direction downwards in Fig. 2.3. Considering the negative sign in Eq. (2.4) the force direction reverses to upwards. This is shown in the figure.

Next, we have to think about the modulus F of the Lorentz force. For the cross product it is equal to the area of the plane spanned by the vectors **v** and **B**:

$$F = \mathrm{e} \cdot v \cdot B \cdot \sin \sphericalangle (\mathbf{v}, \mathbf{B}). \tag{2.5}$$

We realise: There is no force on electrons having a parallel direction of velocity and magnetic field. In other words: A homogeneous magnetic field parallel to the optical axis does not influence electrons which run in the direction of the optical axis (these are "parallel rays" in geometric optics). For the lens effect we need a component of the magnetic field perpendicular to the movement direction of the electrons, i.e. we need an inhomogeneous magnetic field.

For the further discussion it is useful to introduce a coordinate system into the magnetic lens. Because of the rotational symmetry we select cylindrical coordinates r, φ und z (Fig. 2.4).

We realise that the field lines do not have any component in the azimuthal (φ) direction but only such ones in r- (B_r) and z-direction (B_z). The consequences for our parallel ray mentioned above should be explained with the help of Fig. 2.5. It can be seen from this figure that our electron that symbolised the parallel ray is really deflected to the optical axis (Sect. 10.4).

Thereby we recognise two essential properties of the rotational-symmetric magnetic electron lens:

1. Due to the azimuthal velocity component the electrons move on spiral paths with changing distances to the middle (optical) axis through the lens, i.e. the image is rotated against the object. In the following figures with beam paths the $r(z)$-plane is always drawn for easier understanding of the sketches.
2. The degree of the field inhomogeneity, i.e. the ratio B_r / B_z at each position within the lens field (shape of the field lines) essentially determines the refraction prop-

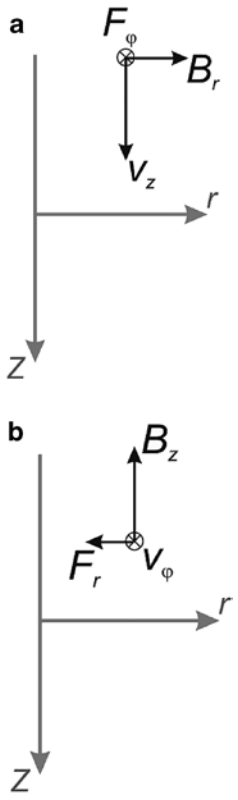

Fig. 2.5 Movement of an electron within an inhomogeneous magnetic lens field. (**a**) The electron has only a component v_z of the velocity ("parallel ray"). Due to the radial component B_r of the magnetic induction a Lorentz force F_φ in azimuthal direction (i.e. into the drawing plane), acts on the electron and causes a velocity component v_φ in azimuthal direction. (**b**) Due to the new velocity component v_φ given now, the electron interacts with the axial component B_z of the magnetic induction and experiences a force directed towards the optical axis as expected for a lens

erties of the lens. Later on (Sect. 2.7.3) we will see that the specimen is positioned within the magnetic field of the objective lens. A specimen of magnetic material changes the field inhomogeneity in dependence on the exact position of the specimen. Therefore, we have to expect some additional difficulties when imaging such magnetic specimens.

2.3 Lens Aberrations

The next question is whether it is possible to set the "right" degree of the field inhomogeneity for lens refraction not only in principle but also for an aberration-free optical imaging. Or transferred to the light optics: What happens if we cannot fulfil the requirement of equal optical distances for all the imaginable waves between object and image point (cf. Sect. 1.2) since the shape of the glass lens is wrong?

In fact, this is a problem for rotational-symmetric electron lenses described here. With perpetuation of the rotational symmetry it is impossible to shape the field inhomogeneity as necessary for aberration-free imaging. This problem was identified

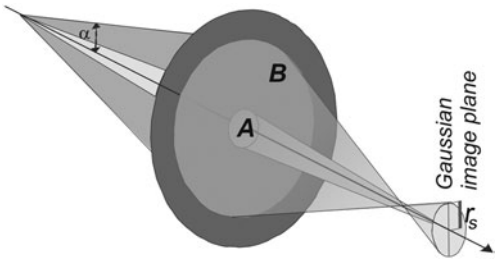

Fig. 2.6 Effect of the spherical aberration. The slightly opened ray bundle *A* creates the image point in the Gaussian image plane. On the other hand, the wider opened (angle α) bundle *B* is refracted stronger. As a consequence, within the Gaussian image plane a spherical aberration disk with radius r_S is created

by Otto Scherzer[2] already in 1936 [1]. As consequence the lens aberrations play a more important role in electron-optical devices than in light optical ones. Here, we want to deal with three important aberrations: the spherical aberration, the chromatic aberration, and the astigmatism.

Spherical aberration This aberration acts especially on rays with larger distances from the optical axis. The name already points to the reason for this aberration: The surface of the lens does not have the right "spherical" shape, it is not properly cut. Or, transferred to magnetic electron lenses, the field shape ("field inhomogeneity") does not meet the requirements for an aberration-free imaging (Sect. 10.4). The discrepancies between requirement and reality are the larger the weaker the rotational-symmetric magnetic field is. Commonly, the spherical aberration of lenses with larger focal lengths ("weak lenses") is larger than that of strong lenses.

The consequence of this "wrong" field shape is shown in Fig. 2.6.

The radius r_S of the spherical aberration disk depends on the opening angle α. Within the Gaussian[3] image plane r_S is given by

$$r_S = M \cdot C_S \cdot \alpha^3 \tag{2.6}$$

with C_S as spherical aberration coefficient of the lens and M as magnification at the imaging plane. The spherical aberration coefficient can be seen as a parameter of the lens quality. For rotational-symmetric magnetic lenses its value is approximately equal to the focal length.

Normally, aberration disks are referred to the object plane. There the radius is:

$$\delta_S = C_S \cdot \alpha^3. \tag{2.7}$$

[2] Otto Scherzer, German physicist and electron optician, 1909–1982

[3] Carl Friedrich Gauß, German mathematician and physicist, 1777–1855

This is independent of the magnification and just relates to the spherical aberration. Because of the dependence of the size of the aberration disk on the cube of the opening angle of the beam the spherical aberration is called aberration of third order.

Chromatic aberration From Eq. (2.4) for the Lorentz force we can see that the force on the electron depends on the magnetic induction and on the velocity of the electron. On the other hand, we know in the meantime that the electron wavelength λ is determined by the electron energy, i.e. by the velocity (cf. Eqs. (1.15)—(1.17)). Different wavelengths but also, of course, different field strengths lead to different optical powers of the magnetic lens and lead to the chromatic aberration. Similar to the spherical aberration within the Gaussian image plane an aberration disk is created with radius δ_C (referred to the object plane) depending on the opening angle α, on the relative fluctuation $\Delta S/S$ of the optical lens power, and on the chromatic aberration coefficient C_C:

$$\delta_C = C_C \cdot \frac{\Delta S}{S} \cdot \alpha. \tag{2.8}$$

There are two reasons for the fluctuation of the optical lens power: Changes of the velocity of the electrons (their wavelength, respectively) and changes of the magnetic lens field. For a plausible explanation we look at the squares of velocity and magnetic induction. The square of the velocity of the electrons is proportional to the electron energy (cf. Eq. (1.16)) and the magnetic induction is proportional to the coil current I (Ampere's[4] law). Because of the increasing optical lens power S by increase of the magnetic field and by smaller electron energy we can write:

$$S \propto \frac{I^2}{\mathrm{e} \cdot U}. \tag{2.9}$$

For small changes ΔS one yields:

$$\left|\frac{\Delta S}{S}\right| = 2 \cdot \left|\frac{\Delta I}{I}\right| + \left|\frac{\Delta U}{U}\right|. \tag{2.10}$$

The objective lens is the lens essential for the quality of the imaging. Referring to the chromatic aberration we have to consider mainly the stability of the objective lens current. Fluctuations of the accelerating voltage, the energy spread of the electrons emitted by the cathode, and also inelastic interactions between electrons and specimen (i.e. interactions related to electron energy losses) can be the cause of fluctuations of the electron energy, too.

Let us additionally assume that the chromatic aberration should be irrelevant in comparison to the spherical aberration. That means:

$$\delta_C \ll \delta_S \text{ and } C_C \cdot \left(2 \cdot \left|\frac{\Delta I}{I}\right| + \left|\frac{\Delta U}{U}\right|\right) \cdot \alpha \ll C_S \cdot \alpha^3, \text{ respectively.} \tag{2.11}$$

[4] André-Marie Ampére, French physicist, 1775–1836

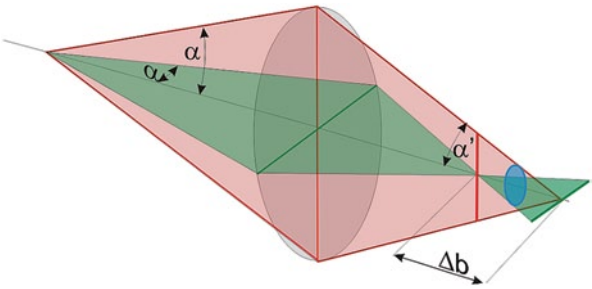

Fig. 2.7 Schematic illustration of a lens with two-fold axial astigmatism

The aberration coefficients C_S und C_C are of the same order, the aperture α amounts to about 10 mrad, therefore the postulation is:

$$2 \cdot \left| \frac{\Delta I}{I} \right| + \left| \frac{\Delta U}{U} \right| \ll 10^{-4}. \tag{2.12}$$

This implies a considerable demand for the stability of the power supply of an electron microscope. For the best state-of-the-art high resolution microscopes equipped with correctors of spherical and chromatic aberrations (cf. Sect. 7.9) a relative stability of $< 10^{-8}$ has to be realised [2].

(Axial) astigmatism In a gedankenexperiment we take two planes from a bundle of electrons which are penetrating a lens (drawn green and red in Fig. 2.7). Astigmatism means that the focal lengths are different in these two (or more) planes.

Deviations from the rotational symmetry created by unroundness of the pole piece bore, by smallest inhomogeneities in the pole piece material, by dirty apertures but also by magnetic material within the lens field can be reasons for these differences. We want to confine ourselves to the two-fold astigmatism as sketched in Fig. 2.7.

The two planes are perpendicular to one another and have got the astigmatic difference of the focal lengths Δf_A connected with difference Δb of the image distances. Obviously, the radius of the (blue drawn) circle of the least confusion is given by:

$$r_{\min} = \frac{1}{2} \cdot \Delta b \cdot \alpha' = \frac{1}{2} \cdot \Delta b \cdot \frac{\alpha}{M} \tag{2.13}$$

with M as magnification. At high magnifications (object distance $g \approx$ focal length f) it follows for (small) differences of the image distances the relation (cf. Eqs. (10.266) and (10.267)):

$$\Delta b = \Delta f_A \cdot M^2. \tag{2.14}$$

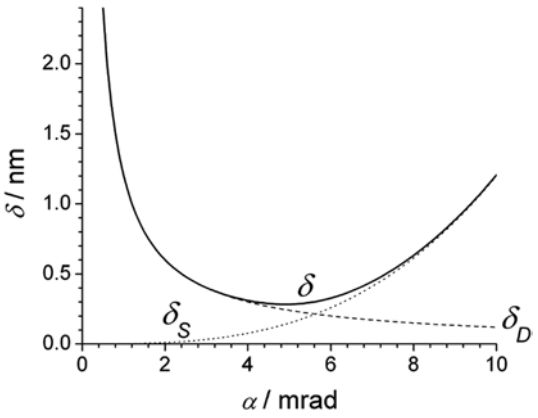

Fig. 2.8 Radius of the spherical aberration disk (δ_S) and the aberration disk by diffraction (δ_D) in the object plane depending on the aperture α (parameter: $C_S = 1.2$ mm, $U_0 = 300$ kV, i.e. $\lambda = 1.97$ pm ≈ 0.002 nm)

Usually, the size of the aberration disk is referred to the object side. Doing that, the radius has to be divided by the magnification M and we get:

$$\delta_A = \frac{r_{\min}}{M} = \frac{1}{2} \cdot \Delta f_A \cdot \alpha. \tag{2.15}$$

2.4 Resolution Limit Considering the Spherical Aberration

At the end of Sect. 1.3 we promised to come back to the resolution limit. Let us remember: Using electron waves we expected a resolution limit of about 2 pm but in reality only about 0.1 nm (i.e. 100 pm) can be reached.

Meanwhile, we recognized a reason of this discrepancy: In contrast to glass lenses our rotational-symmetric magnetic lenses have a spherical aberration limiting the resolution additionally to the (wave specific) aberration by diffraction.

We already know how the radii δ_D und δ_S of both aberration disks in the object plane depend on the aperture α (Eqs. (1.9) and (2.7)). With consideration of very small apertures $(\sin\alpha \approx \alpha)$ and of a refractive index $n = 1$ (vacuum) these equations can be written as:

$$\delta_D = \frac{0{,}61 \cdot \lambda}{\alpha} \text{ and } \delta_S = C_S \cdot \alpha^3 \tag{2.16}$$

We see, there is an oppositional dependence of the aberration disk sizes on the aperture α (cf. Fig. 2.8). Therefore an optimal aperture α_{opt} exists for a minimal size δ of the

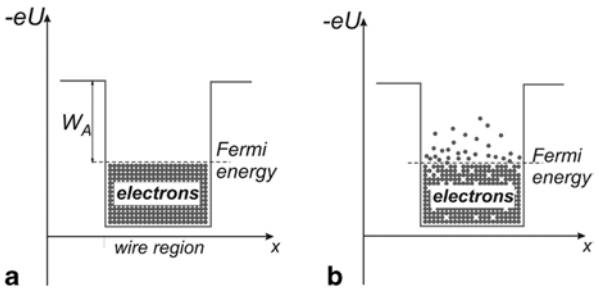

Fig. 2.9 Potential wall model for temperature $T = 0$ K (**a**) and $T > 0$ K (**b**)

resulting aberration disk. For an evaluation of δ we use the law of error propagation:

$$\delta = \sqrt{\delta_S^2 + \delta_D^2}. \tag{2.17}$$

From Fig. 2.8 we read for the minimum of δ: $\alpha_{opt} \approx 5$ mrad and $\delta_{min} \approx 0.3$ nm. The minimum can also be calculated following the equation

$$\delta_{min} = 0.9 \sqrt[4]{C_S \cdot \lambda^3} \tag{2.18}$$

(Sect. 10.5). This value is very close to the resolution limit which is practically reached. But unfortunately, it is a bit too large now. Therefore we need to revisit the resolution limit of a transmission electron microscope once more (Sect. 7.3).

2.5 Electron Gun

Now is the time to think about the possibilities to generate "free" electrons which interact with the specimen and create an optical imaging by lenses.

At first, we have to ask: "Why do the electrons normally run within a wire and do not step out?" The answer is given by the mean positive potential within the wire originated by the atomic nuclei. This potential keeps the electrons within the wire similar to water in a pot. Using this simple model we can easily understand how the electrons can escape the wire: by heating. Assuming we put the water filled pot onto a heat plate then we will see that the water starts to boil and finally the hot water bubbles over the wall of the pot.

In the same manner we can imagine the thermal emission of electrons. Instead of the pot we use a "potential wall model" (Fig. 2.9). The energy levels of the electrons are described by *quantum numbers*. Each level can be occupied by only one electron (Pauli's[5] principle). At the absolute zero of the temperature (0 K = −273.16 °C)

[5] Wolfgang Pauli, Austrian physicist, 1900–1958, Nobel prize in physics in 1945

http://www.springer.com/978-94-017-8600-3

Analytical Transmission Electron Microscopy
An Introduction for Operators
Thomas, J.; Gemming, Th.
2014, XVII, 348 p. 238 illus., 33 illus. in color.,
Hardcover
ISBN: 978-94-017-8600-3